FULL PAPER

Dalton
www.rsc.org/dalton

CF_4 defluorination by Cp_2Ln–H: a DFT study †

Laurent Maron,*[a] Lionel Perrin[b] and Odile Eisenstein*[b]

[a] *Laboratoire de Physique Quantique (UMR 5626), IRSAMC, Université Paul Sabatier, 118 Route de Narbonne, 31062 Toulouse Cedex 4, France. E-mail: laurent.maron@irsamc.ups-tlse.fr*

[b] *Laboratoire de Structure et Dynamique des Systèmes Moléculaires et Solides, (UMR 5636), cc14, Université Montpellier 2, 34095 Montpellier Cedex 5, France. E-mail: odile.eisenstein@univ-montp2.fr*

Received 22nd July 2003, Accepted 5th September 2003
First published as an Advance Article on the web 23rd September 2003

The reaction of CF_4 with Cp_2Ln–H has been studied with DFT(B3PW91) calculations for the entire family of lanthanide elements. The reaction paths for H/F exchange (formation of CF_3H and Cp_2Ln–F) and alkylation (formation of Cp_2Ln–CF_3 and HF) have been determined. Even though a transition state for formation of Cp_2Ln–CF_3 has been located, Cp_2Ln–CF_3 reacts with no energy barrier with HF to give Cp_2Ln–F and CF_3H. The products of the reactions of H/F exchange and alkylation are thus identical. The former reaction is found to be kinetically preferred although the energy barrier is high (>30 kcal mol^{-1}) which suggests that CF_4 would not react with Cp_2Ln–H derivatives. These reactions contrast with that of CH_4 and Cp_2Ln–H for which the energy barrier for the alkylation reaction is lower. The difference in the energy barriers is attributed to an unfavourable charge distribution in the 3c–4e transition state. The structure of Cp_2Ln–CF_3 differs from that of Cp_2Ln–CH_3. Because of the high affinity of Ln for F, CF_3 is dihapto-η^2-C–F bonded. The Ln ··· F interaction is strong and Cp_2Ln–CF_3 can be viewed as an F bridged Ln–CF_2 complex. The presence of a nascent carbene CF_2 group in this complex rationalizes its reactivity with HF.

Introduction

Metal complexes have been used for many years to activate inert bonds either in a stoichiometric or catalytic reaction. A large number of systems are able to activate a C–H bond[1] but many fewer metal complexes successfully activate a C–F bond.[2] It is currently accepted that the strength of the C–F bond is one of the origins of its inertness. For this reason, bis-cyclopentadienyl lanthanides derivatives deserve special attention. The discovery that Cp^*_2Lu–CH_3 (Cp^* = η^5-C_5Me_5) activates CH_4 has had considerable impact on the organometallic community.[3] Furthermore lanthanide elements have a great affinity for fluoride, which suggests that thermodynamic could favour C–F bond activation by formation of a Ln–F bond.

The reaction of Cp^*_2Ln–R (R = H or Me) with a σ bond in molecules like alkanes, arenes, silanes *etc.* can only occur *via* σ bond metathesis because of the absence of any redox reaction. Computational studies of the reaction paths in the case of the reaction of Cp_2Ln–H with H–H,[4] H–CH_3[5] and H–SiH_3[6] reveal some unusual aspects of the σ bond metathesis. The diamond type transition state does not have four relatively similar angles. The diamond is significantly distorted with an almost linear geometry for the R–X–Y moiety where X–Y is reactant (**1**). This is because the 4 electrons involved in the metathesis are entirely located on the R–X–Y part, which is best viewed as a 3c–4e $[R–X–Y]^-$ anionic species in the vicinity of a $[Cp_2Ln]^+$ cation. An unsymmetrical X–Y, like H–CH_3 or H–SiH_3, makes the energies of the topologies R–X–Y or R–Y–X potentially very different, depending on X and Y. A large difference in the energies between the two transition states has been found for CH_4. The transition state with CH_3 in the vicinity, α to the lanthanide (R–X–Y = H–H–CH_3), **2**, is considerably favoured compared to the transition state where CH_3 is β to Ln (R–X–Y = H–CH_3–H), **3**, We have noticed that the height of the energy barrier is related to the ability of the 3c R–X–Y species to stabilize 4 electrons. The 4 electrons being located preferably on the outside atoms or groups of the 3c system, that is on R and Y, these atoms or groups must have the ability to stabilize a negative charge. The central atom of group X must have the ability to be positively charged and to accommodate partial bonding to R *and* Y, which is to become *hypervalent*. As a consequence, the transition state in which R–X–Y = H–CH_3–H, **3**, is highly unfavourable compared to R–X–Y = H–H–CH_3, **2**, (which is accessible in energy) whereas the transition states for R–X–Y = H–SiH_3–H and H–H–SiH_3 are close in energy and energetically accessible. An interesting question that arises is thus the case of CF_4. F is very electronegative and can thus ideally be at the Y site. In addition, the three F of the CF_3 can favour the formation of an hypervalent C at the X site, although it is unclear if they can stabilize a positive charge at C. Finally, all lanthanide elements have a very strong affinity for F, which can drive the thermodynamic of the reaction towards formation of Cp_2Ln–F and CF_3–H, despite the large bond dissociation energy of C–F itself, around 130 kcal mol^{-1}.[7] In addition, it would also be interesting to know if the product of alkylation (formation of Cp_2Ln–CF_3) is feasible because it may not be stable in presence of HF which is made *in situ*. We have thus studied with a DFT method the reactivity of Cp_2Ln–H with CF_4 for the entire family of Ln elements. In the previous studies we have found very little influence of the nature of Ln element. However due to the very different nature of the reactant compared to those studied previously (H_2, CH_4, SiH_4), we thought that it was wiser to study the entire Ln family.

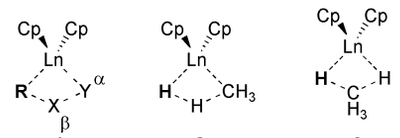

1 **2** **3**

† Electronic supplementary information (ESI) available: Selected DFT calculated bond lengths and angles (Tables S1 to S3) and energy profiles for all lanthanide elements (Table S4). See http://www.rsc.org/suppdata/dt/b3/b308433g/

DOI: 10.1039/b308433g

The activation of the C–F bond has been studied with computational methods for late d transition metals[8] and also for early d transition metals[9] or alkaline or rare earth elements.[10,11] It should be pointed out that these contributions include theoretical studies of reactions in highly varied conditions. Some of these studies mimic reactions occurring in solutions with a metal complex fully surrounded by ligands. Other studies are concerned with a naked metal mimicking a reaction occurring in a laser field. In particular the reaction[10] of Nb^+ where Nb is initially in a +I oxidation state before being oxidized to the more stable +III is very different from what occurs when $Cp_2Ln–R$ reacts in a non-redox process. Some other theoretical studies attempt to study idealized model systems to extract the key features of C–F activation. The key point that emerges from these studies is that the activation of a C–F bond may be kinetically challenging even if it is thermodynamically favourable because the strong C–F bond may be more than compensated by a strong M–F bond. The bonding energy of Ln–F being especially large, it is worth studying if this could impact on the energy barrier. It should be pointed out before entering the description of our results that no reaction of lanthanocene hydride derivative with CF_4 has been reported, despite some attempts by R. A. Andersen.[12]

Computational details

In previous studies[13] we have shown that large core Relativistic Effective Core Potentials (RECPs) optimized by the Stuttgart–Dresden group[14] are well adapted to the calculations of the geometries of lanthanide complexes because the 4f electrons do not participate explicitly in the Ln–X bonds. Different RECPs, one per oxidation state, represent each lanthanide element. The basis sets adapted to the different RECPs augmented by an f polarisation function (α = 1.000) have been used. F has also been represented by an RECP[15] with the associated basis set augmented by two contracted d polarisation gaussian functions (α_1 = 3.3505 (0.357851), α_2 = 0.9924 (0.795561)).[16] C and H have been represented by an all-electron 6-31G(d,p) basis set.[17] Calculations have been carried out at the DFT(B3PW91) level[18] with Gaussian 98.[19] The calculations of BDE have been carried out by optimizing spin doublet at the unrestricted level (the spin contamination has been found to be negligible). The geometry optimizations have been carried out without any symmetry restrictions. The nature of the extrema (minimum or transition state) has been established with analytical frequencies calculations and the intrinsic reaction coordinate (IRC) has been followed to confirm that transition states connect to reactants and products.

Results and discussion

Two reactions have been considered. In eqn. (1), H and F are exchanged between the lanthanide centre and the organic molecule. In eqn. (2), the transfer of the CF_3 group to the metal center corresponds to an alkylation.

$$Cp_2Ln–H + F–CF_3 \longrightarrow Cp_2Ln–F + H–CF_3 \qquad (1)$$

$$Cp_2Ln–H + F–CF_3 \longrightarrow Cp_2Ln–CF_3 + HF \qquad (2)$$

Neutral $Cp_2Ln–H$ corresponds to Ln^{III}, which is the usual stable oxidation state for all lanthanide elements. However, the oxidation state IV is accessible for Ce and the oxidation state II for Eu and Yb. Calculations for $[Cp_2Ce–H]^+$ and $[Cp_2Eu–H]^-$ and $[Cp_2Yb–H]^-$ have thus been carried out in order to study the influence of the oxidation state of the metal on the activation processes. Test calculations have confirmed that neutral $Cp_2Ce–H$, $Cp_2Eu–H$ and $Cp_2Yb–H$ behave like the other neutral complexes. As a consequence, we report only the results for Ce^{IV}, Eu^{II} and Yb^{II} and Ln^{III} for all other lanthanide elements. All numerical values discussed in the text and the optimized structures shown in the figures are for La because they are representative of the results for all Ln^{III} complexes. When necessary the numerical values for Ce^{IV}, Eu^{II} and Yb^{II} are presented.

Geometry of reactants and products

The geometry of the reactant $Cp_2Ln–H$, **4**, has been previously discussed[4] and only the features essential for comparison with the $Cp_2Ln–F$ products are summarized here. The geometry of $Cp_2Ln–H$ varies very little with Ln (see ESI, Table S1).† The structure of $Cp_2La–H$ is shown in Fig. 1. The pyramidalization at Ln has previously been discussed.[20] The lanthanide contraction is calculated to be 0.170 Å.

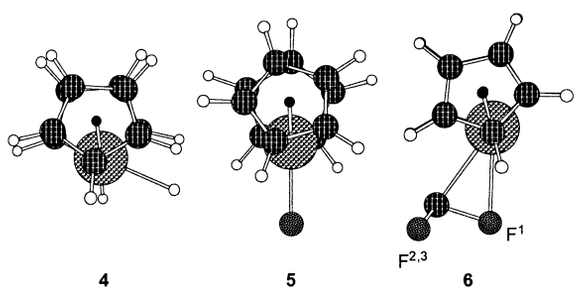

Fig. 1 DFT(B3PW91) optimized structures of $Cp_2La–H$, **4**, $Cp_2La–F$, **5**, $Cp_2La–CF_3$, **6**.

The geometry of the product $Cp_2Ln–F$, **5**, is given in the ESI (Table S1)† and shown for La in Fig. 1. For a given lanthanide, the Ln–F bond is longer than Ln–H by only 0.035 Å. This is rationalized by the large ionic radius of F^- and by the strong Ln–F bonding. An analysis of the topology of the charge density exploiting the "Atoms In Molecule" (AIM) approach[21] of the $Cp_2La–H$ and $Cp_2La–F$ (Fig. 2) illustrates the ionic aspect of the La–X bond ($\Delta\rho(Rc) > 0$) which is larger for La–F, $\Delta\rho(Rc)_F = 3.909\ 10^{-1}$ e Å^{-5}, than for La–H $\Delta\rho(Rc)_H = 6.54\ 10^{-2}$ e Å^{-5}. The pyramidalization at Ln in $Cp_2Ln–F$ is less pronounced than in $Cp_2Ln–H$ as already noticed due to additional $5d_{Ln}/2p_F$ bonding in the fluoride complexes.[20] The lanthanide contraction for Ln–F is equal to 0.176 Å.

The geometry of $Cp_2Ln–CF_3$, **6**, (Table 1, Fig. 1) is very different from the hydrogenated equivalent $Cp_2Ln–CH_3$.[5] Because of the high affinity of d^0 metals for electronegative atoms, the CF_3 group does not make a σ bond with Ln like CH_3 does but is η^2 bonded *via* one C–F bond. As a consequence the local pseudo-C_3 axis of CF_3 is not directed towards the metal center. A similar but much smaller distortion was noticed in $Cp_2Ln–SiH_3$ where Si–H was found to be α agostic.[6] The following numerical values, given for La, illustrate the bonding of CF_3 to the metal center. The C–F^1 bond is longer (1.512 Å) than the two other C–F bonds (1.343 Å) but is short enough to suggest that the presence of a bond. The Ln–F^1 is also significantly formed (2.569 Å) but still much longer than in $Cp_2Ln–F$ (2.179 Å). The sum of the angles La–C–F^2, La C–F^3 and F^2–C–F^3 is equal to 356.7° which indicates the presence of a CF_2 group bonded to La through the HOMO of the singlet CF_2 carbene group. A similar geometry has been found for $[Cp_2Zr–CF_3]^+$.[9] An AIM analysis of the topology of the charge density for $Cp_2La–CH_3$, $Cp_2La–SiH_3$ and $Cp_2La–CF_3$ illustrates the increasing interaction of La with the β atom (Fig. 2). In the case of CH_3 where no La ··· H interaction is present, the C–H bond critical point is along the C–H direction. In the case of SiH_3, the Si–H bond critical point, as well as that for La–Si but in a minor way, is deviated away from the Si–H direction towards La, consistent with the presence of an α Si–H agostic interaction. In the case of CF_3, three critical points characteristic of the La–C, C–F^1 and La–F^1 bonds are present in

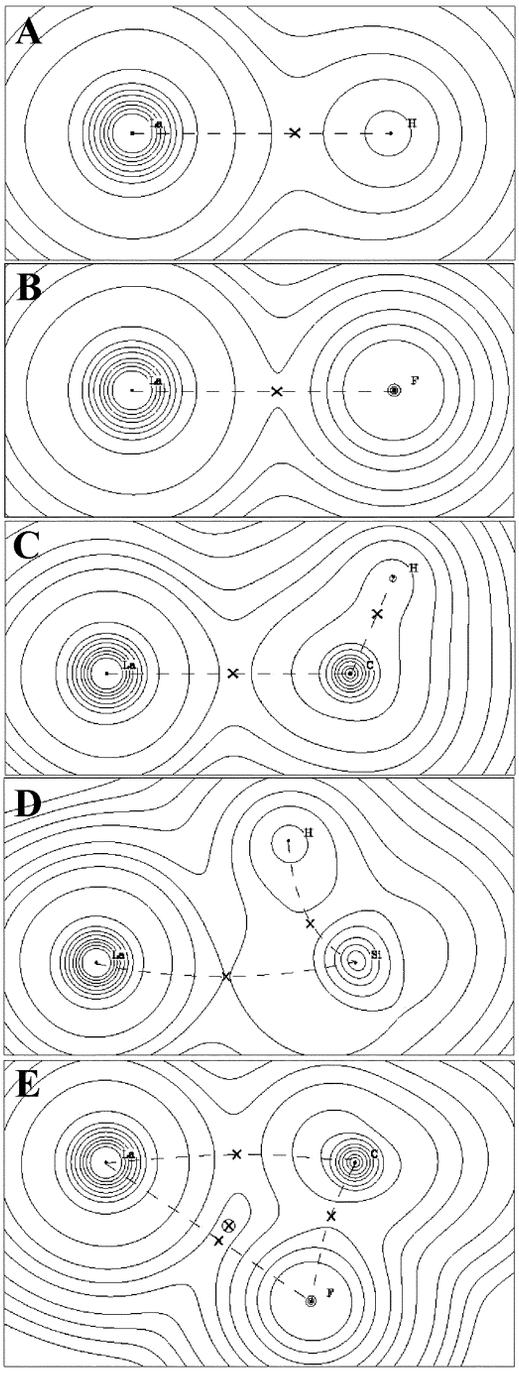

Fig. 2 Topology of the charge density using the AIM methodology for $Cp_2La–H$ **A**, $Cp_2La–F$ **B**, $Cp_2La–CH_3$ **C**, $Cp_2La–SiH_3$ **D**, $Cp_2La–CF_3$ **E**. Crosses show the presence of a bond critical point. The cross in a circle in **E** shows the existence of a cyclic critical point.

addition to a cyclic La–C–F[1] point.‡ Consequently the analysis of the geometry and of the topology of the charge density suggests that $Cp_2Ln–CF_3$ should be viewed as an F bridged $Ln–CF_2$ complex. One can alternatively consider this complex as having a CF_2 bridged La–F bond. Both viewpoints highlight the presence of a CF_2 group, which uses the lone pairs of the other F for additional stabilization because of the inability of La^{III} to back-donate electrons into the empty p orbital of the carbene group. As will be shown the presence of a carbene group in $Cp_2Ln–CF_3$ will be key to the rationalizing of the reaction paths.

‡ Calculation of the topology of the charge density by the AIM method has been carried out for agostic C–H bonds in various systems. In no case was a critical point characteristic of a bond between the metal centre and the H or C ever found. For key references, see: A. Haaland, W. Scherer, K. Ruud, G. S. McGrady, A. J. Downs and O. Swang, *J Am. Chem. Soc.*, 1998, **120**, 3762; W. Scherer, T. Priermeier, A. Haaland, H. V. Volden, G. McGrady, A. J. Downs, R. Boese and D. Bläser, *Organometallics*, 1998, 17, 4406; W. Scherer, P. Sirsch, D. Shorokhov, G. S. McGrady, S. A. Mason and M. G. Gardiner, *Chem. Eur. J.*, 2002, **8**, 2324; G. S. McGrady and A. J. Downs, *Coord. Chem. Rev.*, 2000, **197**, 95.

H/F exchange

The reaction has been represented by eqn. (1). The energy profile is shown for Ln = La in Fig. 3 and given for all metal centers in Fig. 4. Three intermediates, **4** to **9**, shown in Fig. 5 for La, have been located: $Cp_2Ln–H$ (**4**) makes an adduct $Cp_2Ln–H(CF_4)$, **7**, with CF_4, a transition state **9**, which exchanges H and F, produces **8**, which is an adduct of HCF_3 and $Cp_2Ln–F$ (**5**). The final separated products are thus $Cp_2Ln–F$ and HCF_3.

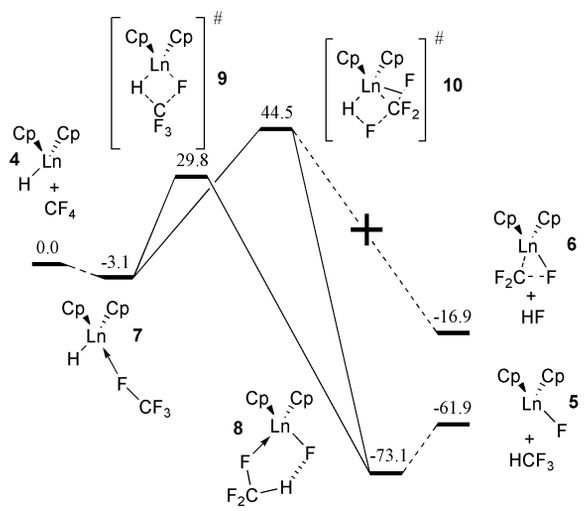

Fig. 3 Energy profiles (kcal mol^{-1}) for H/F exchange (eqn. (1)) and alkylation (eqn. (2)).

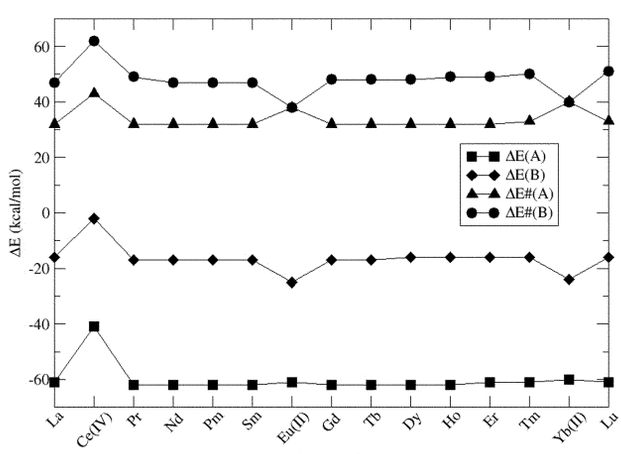

Fig. 4 Evolution of energy of reactions (ΔE_A, ΔE_B) and energy barriers ($\Delta E_A‡$, $\Delta E_B‡$) in kcal mol^{-1} for H/F exchange (eqn. (1)) and alkylation (eqn. (2)) with respect to the lanthanide center.

The CF_4 molecule binds to $Cp_2La–H$ *via* one F of CF_4 (Table S2 of ESI,† Fig. 5). Although the La ··· F–C angle is equal to 146° all other F remain far from La and CF_4 should be viewed as η^1 bonded *via* F in **7**. The La ··· F distance is approximately 0.3 Å longer than La–F in $Cp_2La–F$. The geometry of CF_4 is hardly changed by the coordination as shown by the very small elongation of the coordinated C–F bond (0.039 Å longer than the non-coordinated C–F bonds). The geometry of the $Cp_2La–H$ moiety remains as in the isolated reactant **4** and in particular the hydride remains far from the closest F of CF_4. The bond dissociation energy of CF_4 is very

Table 1 DFT(B3PW91) optimized geometries for $Cp_2Ln–CF_3$, **5**. F^1 is bridging Ln–C (Fig. 1) (distances/Å, angles/°). X is the Cp centroid. All complexes are neutral (Ln^{III}) with the exceptions of $[Cp_2CeX]^+$, $[Cp_2EuX]^-$ and $[Cp_2YbX]^-$, for which the oxidation states of the metal are IV and II and II, respectively

Ln	Ln–C	Ln–F^1	C–F^1	Ln–X	Ln–C–F^1	F^1–C–F^2	X–Ln–X
La	2.576	2.568	1.512	2.549	72.6	105.3	132.8
Ce^{IV}	2.436	2.503	1.475	2.394	75.1	107.7	130.5
Pr	2.540	2.513	1.523	2.505	71.4	105.3	134.1
Nd	2.524	2.487	1.529	2.485	70.9	105.3	134.7
Pm	2.511	2.462	1.536	2.466	70.2	105.4	135.3
Sm	2.497	2.437	1.544	2.448	69.6	105.4	135.8
Eu^{II}	2.708	2.678	1.475	2.650	72.9	102.4	133.7
Gd	2.471	2.390	1.561	2.415	68.4	105.4	136.5
Tb	2.459	2.368	1.570	2.398	67.9	105.5	136.6
Dy	2.446	2.348	1.577	2.382	67.4	105.5	136.8
Ho	2.434	2.330	1.585	2.367	67.0	105.5	136.9
Er	2.421	2.312	1.592	2.352	66.6	105.5	137.0
Tm	2.411	2.296	1.598	2.339	66.3	105.5	137.1
Yb^{II}	2.604	2.606	1.475	2.545	73.6	102.4	135.5
Lu	2.389	2.273	1.605	2.313	66.0	105.5	137.4

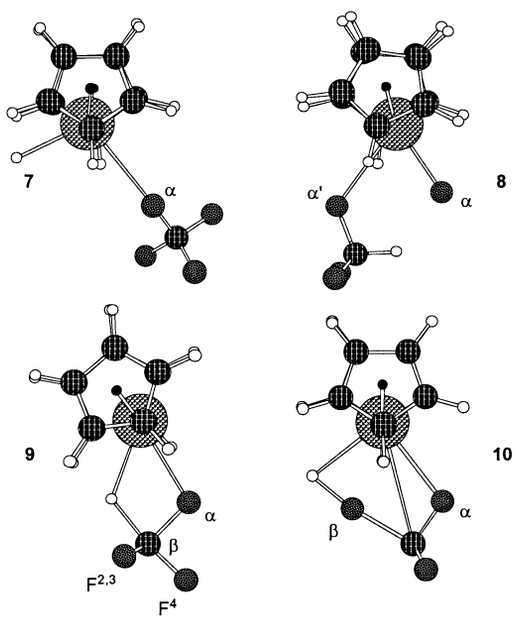

Fig. 5 DFT(B3PW91) optimized structures of $Cp_2La–H(CF_4)$, **7**, $Cp_2La–F(HCF_3)$, **8**, TS for H/F exchange, **9**, TS for alkylation, **10**.

small (3 kcal mol^{-1}). Thus the very large affinity of lanthanide element for F does not manifest itself in the case of CF_4, which reflects probably on the strength of the C–F bond and the lack of a permanent dipole in CF_4. The bond between $Cp_2La–H$ and CF_4 is mostly electrostatic (induced dipole in CF_4) with a minor donor–acceptor interaction as shown by the tiny total NBO charge of 0.01 e on the coordinated CF_4.

In the product of reaction $Cp_2La–F(HCF_3)$, **8**, HCF_3 is bonded *via* a single F to $Cp_2La–F$ (Table S3 of ESI, † Fig. 5). The distance La ··· F is significantly shorter than in **7** (2.745 *vs.* 2.870 Å) but still far from that of La–F(fluoride) = 2.219 Å. The La–F–C angle equal to 122.8° is much more acute than in **7** and furthermore H is close to the fluoride (H ··· F = 2.023 Å). The energy of reaction is very large in favour of the fluoride complex: **8** is 70 kcal mol^{-1} lower in energy than **7**. The difference in energy between **4** and **5** of 61.9 kcal mol^{-1} can be directly understood in terms of bond dissociation energy (BDE) for the C–H, La–F, C–F and La–H bonds. Because the BDE of C–F is about 30 kcal mol^{-1} larger than BDE of C–H,[7] La–F is around 90 kcal mol^{-1} stronger than La–H. A direct calculation of the BDEs in **4** and **5** gives a BDE of 142 kcal mol^{-1} for La–F and 67 kcal mol^{-1} for La–H. The bond dissociation energy of HCF_3 in **8** (11.2 kcal mol^{-1}) is larger than that of CF_4 in **7** (3.1 kcal mol^{-1}). This can be due to an increased electrostatic interaction in the case of the $Cp_2La–F$ due to the larger positive charge at La[20] as well as to the additional F^{α} ··· H attraction.

The energy barrier (Table S4 of ESI, † Fig. 4) is calculated to be 30 kcal mol^{-1} above the separated reactants **4** and CF_4, which is indicative of a difficult reaction. This energy barrier does not allow drawing a definite conclusion on the feasibility of reaction because of the uncertainty associated with the model (Cp for substituted cyclopentadienyl group, no solvent *etc.*) and the level of calculation. It is however consistent with the absence of reaction of CF_4 with (1,2,4-Bu^t–C_5H_2)Ce–H.[12] In the transition state **9**, the La–H is elongated by 0.1 Å (Table 2, Fig. 5) and the C–H significantly formed (around 1.5–1.6 Å). The C–F bond to be broken is elongated by around 0.3 Å and the incipient La ··· F only 0.3 Å longer than La–F in $Cp_2La–F$. The carbon center is in a trigonal bipyramidal geometry with one equatorial F and an apical H. The local pseudo-C_3 axis of the untouched CF_3 group is pointing more toward the leaving F than the incoming H. As already mentioned in our previous studies,[5,6] the transition state for such metathesis reaction is best viewed as a nucleophilic addition of $[H]^-$ to CF_4 with the consecutive formation of an hypervalent transient $[HCF_4]^-$ species in the vicinity of a lanthanide cationic center. The difference in the energy barriers for the reactions with H/H exchange with CH_4 and H/F exchange with CF_4 shows that the strength of the bond to cleave does not determine the height of the barrier. The C–F bond in CF_4 is around 20–30 kcal mol^{-1} stronger than the C–H bond in CH_4. Nevertheless the very high barrier (70 kcal mol^{-1}) calculated in the case of CH_4 is 40 kcal mol^{-1} *lower* in the case of CF_4. This is fully consistent with the well-known stabilization of a hypervalent main group element by substitution with electronegative atoms and the presence of F next to a lanthanide centre. Additional stabilization is provided by the interaction of lanthanide center with the nearby negatively charged fluorine center. The very large lowering of the energy from transition state **9** to product **8** is due to the full formation of the Ln–F bond.

The influence of the lanthanide elements on the energy profile (Fig. 4) of this reaction resembles that found previously.[4,5a,6] Leaving aside the case of Ce^{IV}, Eu^{II} and Yb^{II} the energy barrier tends to be lower near the middle of the lanthanide series although this trend is very weak in this case. There is no change in the geometry of the stationary points. Changing to cationic Ce^{IV} or anionic complexes (Eu^{II} and Yb^{II}) gives higher barriers than for neutral Ln^{III} complexes. The energy of reaction is diminished but remains large. This is consistent with the lesser stabilization of a cationic center by an electron-withdrawing atom. Fewer changes are found for the anionic Eu^{II} and Yb^{II} complexes.

Table 2 DFT(B3PW91) optimized geometries for the transition state **9**, for the reaction of H/F exchange (eqn. (1), Fig. 5). The C–$F^{2,3}$ bonds = 1.349 Å, C–F^4 bond = 1.397 Å, F^2–C–F^3 = 120° and H–C–F^4 = 172.3° for all Ln elements (distances/Å, angles/°). X is the Cp centroid. All complexes are neutral (Ln^{III}) with the exceptions of $[Cp_2CeX]^+$, $[Cp_2EuX]^-$ and $[Cp_2YbX]^-$, for which the oxidation states of the metal are IV, II and II, respectively

Ln	Ln–H	Ln–F^α	Ln–C	C–H	C–F^α	H–C–F^α	F^α–C–$F^{2,3}$	X–Ln–X
La	2.214	2.522	3.297	1.535	1.554	82.1	98.6	132.9
Ce^{IV}	2.033	2.248	3.479	2.090	2.089	70.1	116.6	131.0
Pr	2.180	2.470	3.257	1.546	1.564	81.9	98.8	114.5
Nd	2.164	2.446	3.239	1.551	1.568	81.8	99.0	134.9
Pm	2.150	2.424	3.222	1.556	1.572	81.8	99.1	135.4
Sm	2.137	2.403	3.206	1.561	1.576	81.7	99.2	135.9
Eu^{II}	2.346	2.723	3.464	1.700	1.397	84.7	96.3	133.9
Gd	2.111	2.366	3.178	1.570	1.584	81.5	99.5	136.7
Tb	2.097	2.347	3.161	1.573	1.587	81.5	99.5	136.9
Dy	2.084	2.330	3.147	1.577	1.591	81.4	99.7	137.1
Ho	2.071	2.314	3.134	1.581	1.594	81.3	99.8	137.3
Er	2.058	2.298	3.120	1.585	1.598	81.2	99.9	137.5
Tm	2.048	2.284	3.108	1.588	1.600	81.2	100.0	137.6
Yb^{II}	2.272	2.658	3.410	1.649	1.357	82.4	94.5	134.5
Lu	2.027	2.261	3.087	1.591	1.606	81.0	100.1	137.9

Table 3 DFT(B3PW91) optimized geometries of the transition state **10** for the alkylation reaction (eqn. (2), Fig. 5) (distances/Å, angles/°). X is the Cp centroid. All complexes are neutral (Ln^{III}) with the exceptions of $[Cp_2CeX]^+$, $[Cp_2EuX]^-$ and $[Cp_2YbX]^-$, for which the oxidation states of the metal are IV and II and II, respectively

Ln	Ln–H	Ln–F^α	Ln–F^β	C–F^β	H–F^β	Ln–H–F^β	H–F^β–C	X–Ln–X
La	2.389	2.684	2.486	1.911	1.384	77.4	170.4	132.5
Ce^{IV}	2.245	2.523	2.410	2.022	1.206	82.7	166.7	131.7
Pr	2.353	2.636	2.443	1.912	1.387	76.7	170.0	133.2
Nd	2.337	2.615	2.424	1.913	1.388	76.4	169.8	133.5
Pm	2.322	2.594	2.405	1.914	1.389	76.2	169.6	133.8
Sm	2.307	2.575	2.387	1.914	1.391	75.9	169.5	134.0
Eu^{II}	2.503	3.026	2.567	1.824	1.494	75.2	175.6	133.0
Gd	2.282	2.542	2.355	1.914	1.395	75.3	169.3	134.7
Tb	2.267	2.525	2.338	1.916	1.397	75.1	169.1	134.8
Dy	2.254	2.511	2.323	1.916	1.399	74.9	168.9	135.0
Ho	2.241	2.497	2.308	1.917	1.401	74.6	168.8	135.2
Er	2.229	2.484	2.293	1.917	1.403	74.4	168.7	135.4
Tm	2.217	2.473	2.280	1.918	1.405	74.2	168.6	135.5
Yb^{II}	2.410	3.058	2.459	1.838	1.485	74.0	177.1	134.5
Lu	2.198	2.455	2.258	1.919	1.408	73.9	168.5	135.9

Alkylation reaction

The energy profile for the alkylation reaction (eqn. (2)) is also shown on Fig. 3 with numerical values given in Table S4 of the ESI. † The starting point is the adduct **7** previously discussed. A transition state **10** with CF_3 near the metal (α position) and nascent H–F has been located. However, in an unexpected manner, **10** does not lead to Cp_2Ln–CF_3 and H–F. The intrinsic reaction coordinate indicates that **10** connects to Cp_2Ln–F-(HCF_3), **8**, found in the H/F exchange path. This important point will be discussed further.

The geometry of the transition state **10** is given in Table 3 and Fig. 5. The geometry of the transition state is similar to that found for the reactions of Cp_2Ln–H with CH_4 and with SiH_4.[5,6] The La–H is elongated by about 0.2 Å compared to that in Cp_2La–H and the H–F^β–C is essentially linear (170°). However the CF_3 group has one fluorine (F^α) near the metal center and C rather out of bonding distance (La ··· C = 3.408 Å). The F center to transfer (F^β) to H is already far from C (C–F^β longer by 0.6 Å compared to the two spectator C–F bonds) but the distance C–F^α is an order of magnitude less elongated (0.08 Å compared to the two spectator C–F bonds). The H–F bond is partly formed since it is longer by 0.465 Å compared to the free H–F molecule.

The geometry of transition state **10** shows that CF_3 is not significantly bonded to the lanthanide center since it points its local pseudo-C_3 axis towards the departing F and not towards the metal. In a similar way to what we have shown for CH_4 and SiH_4, this reaction is better viewed as a transfer of the atom in the β position (with respect to Ln), here F, between two terminal groups. Using the terminology given at the beginning of this paper, the transition is an anionic $[R–X–Y]^-$ species with R = H, X = F, Y = CF_3. This rationalizes why the energy of the barrier for alkylation is higher than the barrier for H/F exchange and why the former reaction should not be considered as feasible. In the two reactions, a strong C–F bond is cleaved, and in the two reactions a strong bond is made (Ln ··· F or H ··· F) but there is some additional factors that disfavors the transition state **10**: a negative charge is carried by H and CF_3 and a positive charge by the transferred X group, here F in the case of TS **10**. This is clearly a charge distribution inappropriate to the nature of the atoms and groups.

We have mentioned that this transition state does not lead to Cp_2Ln–CF_3 and HF but to Cp_2Ln–F and HCF_3. The bonding in the transition state and in Cp_2Ln–CF_3 gives a rationale for this result. In the transition state **10**, the lanthanide center is closer to F^α than to the carbon center. Just as for Cp_2Ln–CF_3, there is a clear indication that one F is strongly bonded but the carbon is best viewed as being in a CF_2 carbene group. This nascent CF_2 group in the transition state has the ability to insert into H–F. This is what is observed when following the intrinsic reaction coordinate. One sees that the structures of the transition state and the avoided product Cp_2Ln–CF_3 both contain such a CF_2 group, readily able to react by inserting into a σ bond, here that of the non-liberated H–F.

There is no significant influence of the lanthanide in the Ln^{III} family both on the energy profile (Fig. 4) and on the geometry of the stationary points for the alkylation reaction. There are more changes associated with Ce^{IV}. The energy of reaction for formation of $[Cp_2Ce–CF_3]^+$ is considerably smaller than for the

neutral Ln^{III} equivalent. This is associated with the fact that a strongly acceptor group like CF_3 is not so well suited to stabilize a cationic complex. Likewise the energy barrier is also significant higher than in the case of Ln^{III} complexes. The opposite influence is obtained in the case of negatively charged complexes of Eu^{II} and Yb^{II}.

Conclusion

The study of the reaction paths of CF_4 with lanthanocene hydride complexes suggest that a very slow or even no reaction is to be expected between these two reactants despite the very large predicted favorable energy of reaction for formation of a fluoride complex. If a reaction were to occur, the only product would be the fluoride complex and not the trifluoroalkyl complex. A general pattern emerges from the set studies carried out on the reactions of $Cp_2Ln–R$ (R = H, Me) with X–Y equal to H–H, CH_4, SiH_4 and CF_4. In all cases, the transition state contains a negatively charged 3c–4e species $[R–X–Y]^-$ nearby a cationic $[Cp_2Ln]^+$ fragment. The height of the energy barrier can be qualitatively understood by considering the charge distribution in this 3c–4e $[R–X–Y]^-$ species as well as the ability of the central group X to become hypervalent. The barrier for H/H exchange is therefore considerably lower for SiH_4 than for CH_4 because Si has more ability to become hypervalent. We can also rationalize that the H/F exchange in the case of CF_4 has a lower barrier (R–X–Y = H–CF_3–F) than the H/H exchange in the case of CH_4 (R–X–Y = H–CH_3–H) despite the higher bond dissociation energy of C–F compared to C–H. Electronegative atoms like F stabilize hypervalency at C especially at the apical site (Y site) where negative charge can strongly accumulate.

The affinity of lanthanide for F is so large that it makes the geometry of $Cp_2Ln–CF_3$ very different from that of $Cp_2Ln–CH_3$. $Cp_2Ln–CF_3$ is best viewed as a $Ln–CF_2$ unit bridged by F or as La–F bond bridged by CF_2. This shows how a carbene group, in the present case already stabilized by two fluorine atoms, can be further stabilized by the fluoride near the lanthanide center. Probably because of the very large stability of $Cp_2Ln–F$ and the stability of CF_2, characterized as an isolated carbene, a carbene like chemistry emerges from the reaction of eqn. (2) as shown by the insertion of CF_2 into H–F. A similar geometrical situation has been found in Zr^{IV} complex[9] but this study shows how the bonding affects the reactivity. The very strong difference between the reactivity of CH_4 and CF_4 with $Cp_2Ln–H$ suggests that some interesting reactivity could be obtained by combining the low barrier obtained for CH_4 with the strong thermodynamic drive obtained for CF_4. This could be expected should CH_nF_{4-n} be reacted with lanthanide complexes. This is under study in our group.

Acknowledgements

The authors are most grateful to Prof. R. A. Andersen (UC Berkeley) for numerous illuminating discussions and communication of unpublished results. The authors gratefully acknowledge the national French computing centre CINES and the local computing facilities in Toulouse CALMIP for a generous donation of computing time.

References

1 For some recent reviews, see: Activation of Unreactive Bonds and Organic Synthesis, *Topics in Organometallic Chemistry*, ed. S. Murai, Springer, Berlin, 1999, vol. 3; R. H. Crabtree, *Chem. Rev.*, 1995, **95**, 987; C. Hall and R. N. Perutz, *Chem. Rev.*, 1996, **96**, 3125; A. E. Shilov and G. B. Shu'lpin, *Chem. Rev.*, 1997, **97**, 2879; G. J. Kubas, *Transition Metal σ bond and Dihydrogen Complexes*, Kluwer Academic–Plenum Publishers, New York, NY, 2001; G. W. Parshall, *Acc. Chem. Res.*, 1975, **8**, 113; R. H. Crabtree, *Chem. Rev.*, 1985, **85**, 245; B. A. Arndtsen, R. G. Bergman, T. A. Mobley and T. H. Peterson, *Acc. Chem. Res.*, 1995, **28**, 154; J. A. Labinger and J. E. Bercaw, *Nature*, 2002, **417**, 507.

2 For reviews, see for instance: U. Mazurek and H. Schwarz, *Chem. Commun.*, 2003, 1321; T. G. Richmond, *Top. Organomet. Chem.*, 1999, **3**, 243; J. L. Kiplinger, T. G. Richmond and C. E. Osterber, *Chem. Rev.*, 1994, **94**, 373; J. Burdeniuc, B. Jedlicka and R. H. Crabtree, *Chem. Ber./Recl.*, 1997, **130**, 145; T. Braun and R. N. Perutz, *Chem. Commun.*, 2002, 2749; C. J. Burns and R. A. Andersen, *J. Chem. Soc., Chem. Commun.*, 1989, 136.

3 P. L. Watson, *J. Chem. Soc., Chem. Commun.*, 1983, 276; P. L. Watson and G. W. Parshall, *Acc. Chem. Res.*, 1985, **18**, 51.

4 L. Maron and O. Eisenstein, *J. Am. Chem. Soc.*, 2001, **123**, 1036.

5 L. Maron, L. Perrin and O. Eisenstein, *J. Chem. Soc., Dalton Trans.*, 2002, 534; L. Perrin, L. Maron and O. Eisenstein, *C–H Activation, ACS Symposium Series*, eds. A. Goldman and K. Goldberg, ACS, Washington, DC, in press; E. C. Sherer and C. J. Cramer, *Organometallics*, 2003, **22**, 1682.

6 L. Perrin, L. Maron and O. Eisenstein, *Inorg. Chem.*, 2002, **41**, 4355.

7 B. E. Smart, *Mol. Struct. Energy*, 1986, **3**, 141; D. F. McMillen and D. M. Golden, *Annu. Rev. Phys. Chem.*, 1982, **33**, 493; *CRC Handbook of Chemistry and Physics*, 71st edn., CRC Press, Boca Raton, FL, 1990–91.

8 For example, M. D. Su and S.-Y. Chu, *J. Am. Chem. Soc.*, 1997, **119**, 10178; R. Bosque, S. Fantacci, E. Clot, F. Maseras, O. Eisenstein, R. N. Perutz, K. B. Renkema and K. G. Caulton, *J. Am. Chem. Soc.*, 1998, **120**, 12634; K. Krogh-Jespersen and A. S. Goldman, *ACS Symposium Series 721, Transition State Modelling for Catalysis*, ACS, Washington, DC, 1998, 151; H. Gérard, E. R. Davidson and O. Eisenstein, *Mol. Phys.*, 2002, **100**, 533; T. Braun, L. Cronin, C. L. Higgitt, J. E. McGrady, R. N. Perutz and M. Reinhold, *New J. Chem.*, 2001, **25**, 19.

9 L. A. Watson, D. V. Yandulov and K. G. Caulton, *J. Am. Chem. Soc.*, 2001, **123**, 603.

10 R. H. Hertwig and W. Koch, *Chem. Eur. J.*, 1999, **5**, 312.

11 J. N. Harvey, D. Schröder, W. Koch, D. Danovich, S. Shaik and H. Schwarz, *Chem. Phys. Lett.*, 1997, **278**, 391; D. Caraiman, G. K. Koyanagi, A. Cunje, A. C. Hopkinson and D. K. Bohme, *Organometallics*, 2002, **21**, 4293.

12 R. A. Andersen, private communication.

13 L. Maron and O. Eisenstein, *J. Phys. Chem. A*, 2000, **104**, 7140.

14 For Ln^{II} and Ln^{III}, see: M. Dolg, H. Stoll, A. Savin and H. Preuss, *Theor. Chim. Acta*, 1989, **75**, 173; M. Dolg, H. Stoll, A. Savin and H. Preuss, *Theor. Chim. Acta*, 1993, **85**, 441; For Ce^{IV}, see: M. Dolg, P. Fulde, W. Kuechle, C.-S. Neumann and H. Stoll, *J. Chem. Phys.*, 1991, **94**, 3011.

15 A. Bergner, M. Dolg, W. Küchle, H. Stoll and H. Preuss, *Mol. Phys.*, 1993, **80**, 1431.

16 L. Maron and C. Teichteil, *Chem. Phys.*, 1998, **237**, 105.

17 W. J. Hehre, R. Ditchfield and J. A. Pople, *J. Chem. Phys.*, 1972, **56**, 2257.

18 J. J. P. Perdew and Y. Wang, *Phys. Rev. B*, 1992, **82**, 284; A. D. Becke, *J. Chem. Phys.*, 1993, **98**, 5648.

19 M. J. Frisch, G. W. Trucks, H. B. Schlegel, G. E. Scuseria, M. A. Robb, J. R. Cheeseman, V. G. Zakrzewski, J. A. Montgomery, Jr., R. E. Stratmann, J. C. Burant, S. Dapprich, J. M. Millam, A. D. Daniels, K. N. Kudin, M. C. Strain, O. Farkas, J. Tomasi, V. Barone, M. Cossi, R. Cammi, B. Mennucci, C. Pomelli, C. Adamo, S. Clifford, J. Ochterski, G. A. Petersson, P. Y. Ayala, Q. Cui, K. Morokuma, P. Salvador, J. J. Dannenberg, D. K. Malick, A. D. Rabuck, K. Raghavachari, J. B. Foresman, J. Cioslowski, J. V. Ortiz, A. G. Baboul, B. B. Stefanov, G. Liu, A. Liashenko, P. Piskorz, I. Komaromi, R. Gomperts, R. L. Martin, D. J. Fox, T. Keith, M. A. Al-Laham, C. Y. Peng, A. Nanayakkara, M. Challacombe, P. M. W. Gill, B. G. Johnson, W. Chen, M. W. Wong, J. L. Andres, C. Gonzalez, M. Head-Gordon, E. S. Replogle and J. A. Pople, GAUSSIAN 98 (Revision A.11), Gaussian, Inc., Pittsburgh, PA, 2001.

20 L. Perrin, L. Maron and O. Eisenstein, *Faraday Discuss.*, 2003, **124**, 25.

21 R. F. W. Bader, Atoms in Molecules, *Int. Ser. Monogr. Chem.*, 1994, **22**, 1.